17th World Conference on Earthquake Engineering, 17WCEE
Sendai, Japan - September 13th to 18th 2020

PROPORTIONAL VISCOUS DAMPING MODEL FOR MATCHING FREQUENCY-DEPENDENT DAMPING RATIO

C.-L. Lee[(1)]

[(1)] *Senior Lecturer, Dept. of Civil and Natural Resources Engineering, University of Canterbury, chin-long.lee@canterbury.ac.nz*

Abstract

Existing proportional damping models for simulating energy dissipations not already accounted for in hysteretic material models in a large-scale structure are either inaccurate in matching a user-specified damping ratio curve or computationally costly in computing solutions due to having a fully populated damping coefficient matrix. Some also result in spurious damping forces during rigid body motions and at degrees of freedom without mass inertia. A new and efficient proportional damping model based on a bell-shaped basis function and a sparse damping matrix has recently been proposed to address all these problems. It is particularly accurate in matching a constant damping ratio across a wide range of frequencies of interests commonly considered in earthquake engineering practice. However, the basis function of this model has a fixed frequency bandwidth on the logarithmic scale, limiting its usage in matching a frequency-dependent damping ratio that has its values change drastically over a short frequency interval, which is found in a piecewise constant or step distribution of damping ratio.

To address this problem, this paper presents a new model modified from the original model. The proposed modification adjusts the frequency bandwidth of the original basis function by raising the order of the function, while maintaining its bell shape, thereby maintaining all the good features of the original model in avoiding spurious damping forces. Matching and response history analysis examples are reported to demonstrate the accuracy of this modified model in matching a step distribution of damping ratio and in computing the solutions of global and local responses, in comparison to the original model.

Keywords: proportional viscous damping; frequency-dependent; adjustable bandwidth; step distribution; bell shape

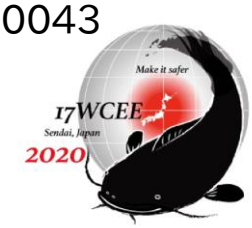

1. Introduction

When a large-scale inelastic structure such as a multi-storey building is subjected to seismic loading, energy dissipations are not only contributed from yielding or damage in structural components such as beams, columns, braces, walls and slabs, but also contributed from friction mechanisms happening in joints, partition walls, ceiling, cladding, interactions between non-structural components and structural components, and others that cannot be easily identified. In numerical modelling, these mechanisms are usually difficult to be explicitly modeled and are commonly accounted for using a viscous damping term in the equations of motion based on the well-known damping matrix **C**. While these mechanisms are unlikely viscous, using an idea of equivalent damping is often considered acceptable [1,2].

Commonly considered damping models include Rayleigh [3], Caughey [4], and Wilson-Penzien [5] because they possess normal modes, allow direct model calibration against experimental data that are often modal based, and fit well to the established knowledge for seismic structural design. With only two terms, the Rayleigh model can match damping ratios of the structure only at two modes, making it unfriendly for model calibration. Its damping ratio curve in the frequency domain grows unbounded at zero and infinite frequencies, resulting in having non-physical damping forces for rigid body modes and at degrees of freedom without mass inertia. Nevertheless, because it gives a **C** matrix that is as sparse as the stiffness matrix **K**, it is computationally very efficient, making it still popular among structural engineer communities despite its many limitations. The Caughey model aims to extend the Rayleigh model to match damping ratios at more modes with more parameters, but results in a dense or even fully populated **C** matrix and the computational efficiency is, thus, compromised. Its model parameters are also obtained using an ill-conditioned matrix, a problem that is solved only recently by Luco [6]. It also has the problem of having non-physical damping forces for rigid body modes and at degrees of freedom without mass inertia. The Wilson-Penzien model forms the **C** matrix directly using the modal matrix, allowing damping ratios to be matched directly at each mode. However, it requires costly computations of natural frequencies and mode shapes, and also results in a dense or fully populated **C** matrix. Nevertheless, computational cost can be reduced via vector-vector multiplication [7]. To overcome high computational cost, elemental damping model was recently developed by forming the **C** matrix from elemental **C** matrices, thereby ensuring a sparse effective stiffness matrix $\mathbf{K}_{\mathbf{eff}}$. Although it fits well to an idea that energy dissipations are contributed from components instead of a system as a whole, normal modes are lost, causing calibration against modal damping ratios difficult.

In view of the above discussions, a new proportional damping model has recently been proposed [8-10]. It has a bell-shaped basis function that allows any smooth damping ratio curve to be matched, while maintaining a zero damping ratio at zero and infinite frequencies, thereby avoiding non-physical spurious forces during rigid body motions and at degrees of freedom without mass inertias. It can also be implemented as a sparse matrix, ensuring low memory storage and high computational efficiency. Several examples have also been conducted to demonstrate its cost efficiency, accuracy, and advantages in addressing the above problems compared to existing models [8-10].

This new model, however, has a fixed frequency bandwidth on the logarithmic scale, limiting its matching capability for a damping ratio curve that changes drastically within a short frequency interval. A drastic change of damping ratio in a short interval could be considered in practice during a case of having a piecewise constant or step damping ratio curve that allows small damping ratios for lower modes and large damping ratios for higher modes. It is, therefore, warranted to propose a change in the model to allow its frequency bandwidth to be adjustable, which is the objective of this study.

In this paper, the original model will first be briefly introduced, followed by the proposed changes and examples demonstrating its versatility in matching a step distribution of damping ratio. Response history analysis examples for demonstrating its accuracy will also be reported.

2. Original Damping Model

The original damping model [8-10] forms a damping ratio curve in the frequency domain using a bell-shaped basis function, denoted as *N*, as defined in Eq. (1).

$$N(\omega;\omega_p) = \frac{2\omega_p\omega}{\omega_p^2+\omega^2} \tag{1}$$

where ω is the circular frequency in the units of radian per second and ω_p is the parameter that controls the location of the peak. The semicolon inside the parentheses indicating that the ω_p is a parameter instead of a variable. This basis function is also plotted in Fig.1.

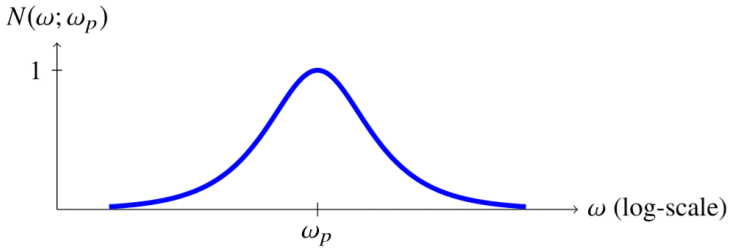

Fig. 1 – Bell-shaped basis function.

By using n_b number of basis functions, with each scaled by another parameter ζ_p, a general damping ratio curve, $\zeta(\omega)$, can be generated, as shown in Eq. (2).

$$\zeta(\omega) = \sum_{i=1}^{n_b} N(\omega;\omega_{pi})\zeta_{pi} \tag{2}$$

Some example curves: constant, linear and trilinear on the logarithmic scale, generated using this basis function are given in Fig.2.

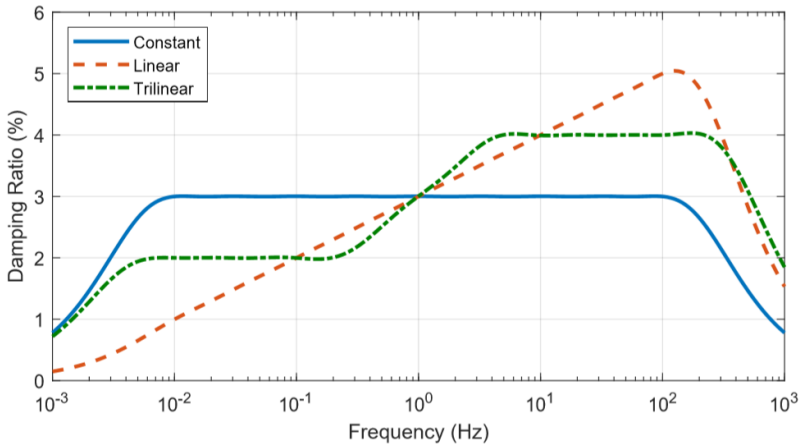

Fig. 2 – Three examples of damping ratio curves generated using the bell-shaped basis functions.

These examples show that the model is quite versatile in producing damping ratio curves commonly considered in response history analysis practice.

The damping coefficient matrix **C** of this model is given in Eq. (3)

$$\mathbf{C} = \sum_{i=1}^{n_b}(\mathbf{M}_{\mathbf{C}i} - \mathbf{M}_{\mathbf{C}i}(\mathbf{M}_{\mathbf{C}i} + \mathbf{K}_{\mathbf{C}i})^{-1}\mathbf{M}_{\mathbf{C}i}), \quad \mathbf{M}_{\mathbf{C}i} = 4\zeta_{pi}\omega_{pi}\mathbf{M}, \quad \mathbf{K}_{\mathbf{C}i} = \frac{4\zeta_{pi}}{\omega_{pi}}\mathbf{K} \tag{3}$$

where **M** and **K** are mass and stiffness matrices, respectively. This **C** matrix does not require **M** nor **K** to be invertible, making it suitable for a structural model with some degrees of freedom without mass inertias and experiencing rigid body motions without non-physical damping forces. Although this **C** matrix is fully populated for the degrees of freedom with mass inertias, it can be implemented as a sparse matrix. Its computational efficiency is in an order much lower than other models that result in a fully populated **C** matrix. In fact, the larger the number of degrees of freedom, the better the computational efficiency [9].

3. Proposed Modification

3.1 Frequency form

The basis function has a fixed frequency bandwidth on the logarithmic scale. The bandwidth, denoted as w_b, is defined as the distance on the natural logarithmic scale between two frequency points, ω_1 and ω_2, that have their function values equal to 0.5. Its definition in terms of formula and value are given in Eq. (4)

$$w_b \stackrel{\text{def}}{=} \ln \omega_2 - \ln \omega_1 = 2 \cosh^{-1} 2 = 2.634 \tag{4}$$

This is a fixed value independent of ω_p only on the logarithmic scale. Should the scale be linear, it would increase linearly with ω_p. The basis function is, therefore, unsuitable for matching a damping ratio curve that changes drastically over a short frequency interval, particularly for a step function that allows a low damping ratio for lower modes. It is particularly worse when the step change occurs at a high frequency.

This study proposes to adjust this bandwidth by raising the order of the basis function, such that the new basis function, denoted as N_1, is defined in Eq. (5).

$$N_1(\omega; \omega_p, n_p) = \left(\frac{2\omega_p \omega}{\omega_p^2 + \omega^2} \right)^{2n_p+1} \tag{5}$$

where n_p is the parameter that adjusts the order of the basis function. Note, the parameter n_p can only be an integer (to be discussed later). With this new parameter, the corresponding bandwidth of the new basis function is given in Eq. (6).

$$w_b(n_p) = 2 \cosh^{-1} \left(\sqrt[2n_p+1]{2} \right) \tag{6}$$

The modified basis functions for different values of n_p, using a normalized variable $\omega_r = \omega/\omega_p$, are plotted in Fig. 3. This figure shows that the higher the value of n_p, the smaller the bandwidth.

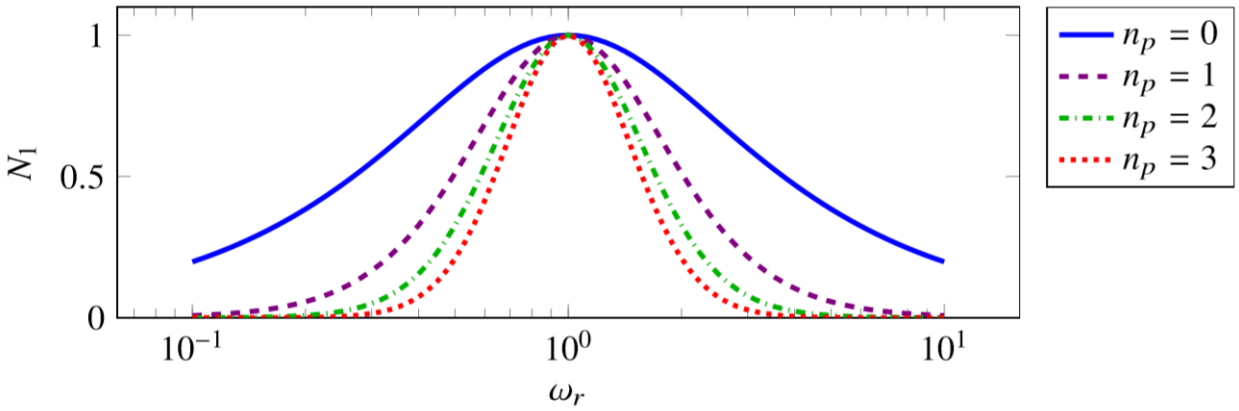

Fig. 3 – New basis functions parameterized with different values of n_p.

The bandwidth w_b versus the parameter n_p is plotted in Fig. 4, which shows that the bandwidth is decreasing with increasing n_p. The rate of decrease becomes smaller and smaller, nonetheless.

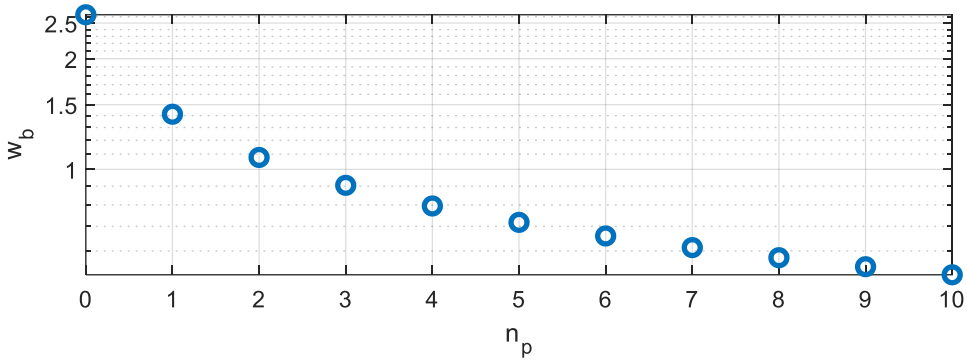

Fig. 4 – Bandwidth w_b versus n_p of the new basis function.

2.1 Matrix form

The modified model has the following expression of the **C** matrix using one basis function of order n_p.

$$\mathbf{C}(n_p) = \mathbf{M_C}(2\mathbf{A_C})^{-1}\mathbf{K_C}\left(\mathbf{A_C}^{-1}\mathbf{M_C}\mathbf{A_C}^{-1}\mathbf{K_C}\right)^{n_p}, \quad \mathbf{A_C} = 0.5(\mathbf{M_C} + \mathbf{K_C}) \tag{7}$$

Note, it is clear from Eq. (7) that the parameter n_p can only an integer, since computing a matrix with a fractional exponent would require a special algorithm that is not computational cheap and feasible for a response history analysis.

This **C** matrix can be freely combined through addition with other **C** matrices of different n_p's to form a general expression of a **C** matrix using multiple basis functions. Similar to the original **C** matrix given in Eq. (3), it does not require **M** nor **K** to be invertible, making it still suitable for structures that have some degrees of freedom without mass inertias and that experience rigid body motions or collapse mechanisms. Nevertheless, the matrix $\mathbf{A_C}$ must be invertible. It is, fortunately, often the case for a dynamically stable structure.

This **C** matrix is also dense or even fully populated, but it can be implemented as a sparse matrix, thereby maintaining a similar order of the computational cost during response history analysis. The idea of this sparse matrix implementation is based on the work done previously by the same author [9]. Given that the discussion would be quite intensive and is beyond the scope of this paper, it will not be discussed further. Interested readers could refer to the referenced paper. Note, the computational cost will increase with increasing n_p. It is, therefore, advisable to use an n_p as small as possible so long as matching quality is acceptable.

4. Matching of Step Distribution

A constant damping ratio curve is common in response history analysis [7,11]. However, it may be desired to have a step distribution such that a lower damping ratio is used for lower modes. The following shows an example on evaluating the accuracy of the original damping model and the proposed modified model in matching this distribution.

In this example, the damping ratio is constant at 2% for frequencies between 0.01 Hz and 1 Hz, and at 5% for frequencies between 1 Hz and 100 Hz. Fig. 5 shows the generated curves using the original model and the modified model. Five basis functions are used in both models. For the modified model, only the middle basis function has its order raised by the parameter n_p while all other basis functions have their n_p's equal to zero. The value of n_p of the middle basis function is either 1 or 5. This is to demonstrate how the slope at the transition is adjusted by n_p. Table 1 shows the parameters used for each model.

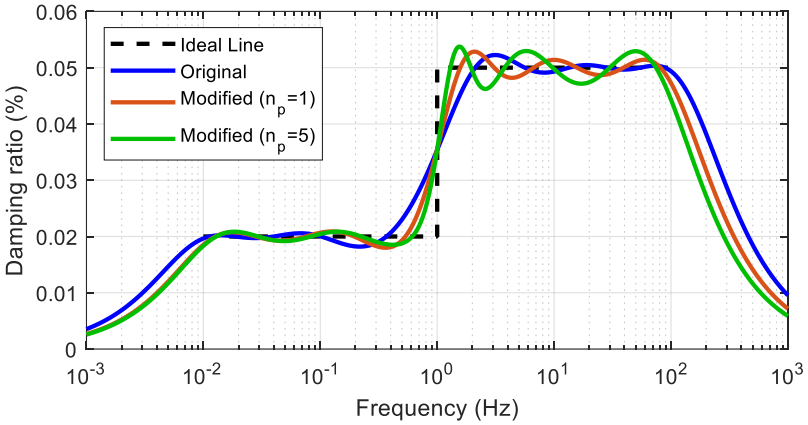

Fig. 5 – Step curves generated using the original (blue) and modified (red) models.

Table 1 – Parameter values for the curves shown in Fig. 5.

Original		**Modified (n_p = 1)**		**Modified (n_p = 5)**	
ω_p	ζ_p	ω_p	ζ_p	ω_p	ζ_p
rad./s	**%**	**rad./s**	**%**	**rad./s**	**%**
0.0099	1.58	0.0141	1.72	0.0146	1.74
0.0771	1.36	0.1445	1.59	0.1473	1.45
2.414	4.13	1.737	3.14	1.431	2.36
17.79	2.74	8.522	3.97	4.857	4.42
111.1	3.81	78.40	4.17	60.54	4.51

Fig.5 shows that the original model with a fixed bandwidth cannot produce a step curve with a sharp transition. The transition can only gradually take place with a gentle slope across the interval between 0.4 Hz and 2 Hz. If there is any structural frequency falls within this transition interval, its corresponding damping ratio will be compromised by having a number between 2% and 5%. This large transition interval limits the application of the original model to structures with closely spaced structural frequencies near the transition.

In comparison, the modified model with an adjustable bandwidth could produce a steeper transition, and the slope is steeper with a higher n_p. This transition interval can be further minimized by having more and more basis functions with a narrower bandwidth (using a higher n_p) near the transition.

Note, there are ripples in the curves near the transition. They cannot be avoided given the bell-shaped nature of the basis function. It is like a Gibbs phenomenon [12, 13] when a discontinuous function is produced by summing multiple continuous functions. Nevertheless, they can be controlled to stay within an acceptable tolerance by having more basis functions with a smaller bandwidth.

The comparison in this example shows that the proposed modified basis function has great potential in matching a curve with drastic changes in the curve over a short frequency interval.

5. Response History Analysis Example

The accuracy of the proposed modified model in representing a step distribution of damping ratio is evaluated in a response history analysis. The structure considered is a one-bay eight-storey steel moment-resisting frame (MRF). The diagram of this structure is shown in Fig. 6.

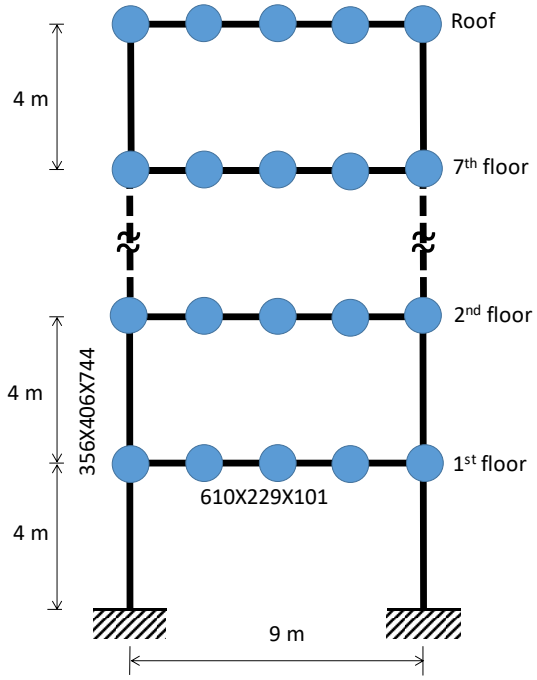

Fig. 6 – Diagram of steel moment-resisting frame.

The sections used for the beams and columns are 610X229X101 and 356X406X744, respectively. The material used for these steel sections is of grade 250 with a yield strength of 250 MPa. Each beam is modelled with four one-component models [14] without axial moment interaction. Each column is modelled with a plastic-hinge element that has axial-moment interaction incorporated with a yield surface without strain-hardening.

In each floor, the gravity load is 22.5 kN/m, the seismic mass is 12.75 tonne/m for horizontal motions and is 6.37 tonne/m for vertical motions. All the mass is lumped at nodes with horizontal and vertical masses only (see Fig.6). With these masses, the first five structural frequencies are 0.36 Hz, 1.23 Hz, 2.51 Hz, 4.30 Hz, and 5.82 Hz.

The damping ratio curve in the frequency domain is a step function with the transition at 1 Hz. The damping ratio is 2% for frequencies below 1 Hz and is 5% for frequencies above 1 Hz. In other words, a lower damping ratio at 2% is considered for the first mode, while a higher damping ratio at 5% for all the higher modes.

Three damping models are considered: the Wilson-Penzien model, the original model, and the modified model. The parameters of these models are all calibrated to produce the step damping ratio distribution. In the Wilson-Penzien model, the damping ratios at the modes with natural frequency less than 20 Hz are matched to the step distribution, while all other higher modes are not matched. These modes are selected such that the total effective modal mass is at least 95%. Three and five basis functions are used for the original and modified models, respectively. In the modified model, the middle basis function has its n_p equal to 5, and the 2nd and the 4th basis functions have their n_p's equal to 1. The 1st and the 5th basis function have their n_p's equal to zero. Fig. 7 shows the damping ratio curves of these models. It shows that, with a gentler slope, the original model has the second mode matched to a damping ratio at about 4%, with an error of 20%. The damping ratios of other modes are generally matched to the correct values with an acceptable error by all three models.

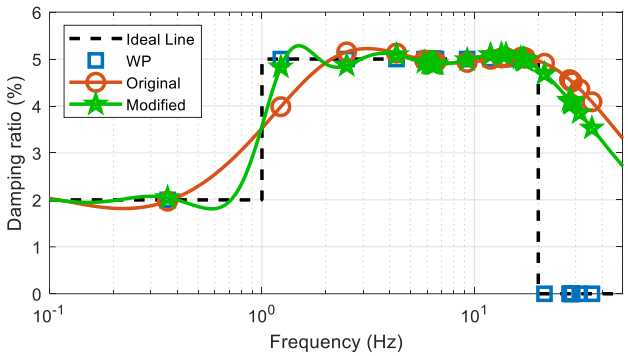

Fig. 7 – Damping ratio curves (markers highlight damping ratio at each mode, but not all are shown).

The input motion is Component 1 of the record NGA0779, recorded during the 1989 Loma Prieta earthquake. The peak ground acceleration is scaled to 1g. The analysis was conducted on FEDEASLab [15] using the Newmark method with average acceleration. The damping coefficient matrix is assumed to stay constant throughout the duration of analysis, in accordance to the suggestion by Chopra and McKenna [7].

The roof displacement time histories are shown in Fig.8. There is almost no difference in the roof displacement among using the three damping models. This is because it is governed mainly by the first mode, and all models give nearly the same damping ratio for this mode. Nevertheless, the displacement resulted from using the original model does show some small differences when time is beyond 12 sec.

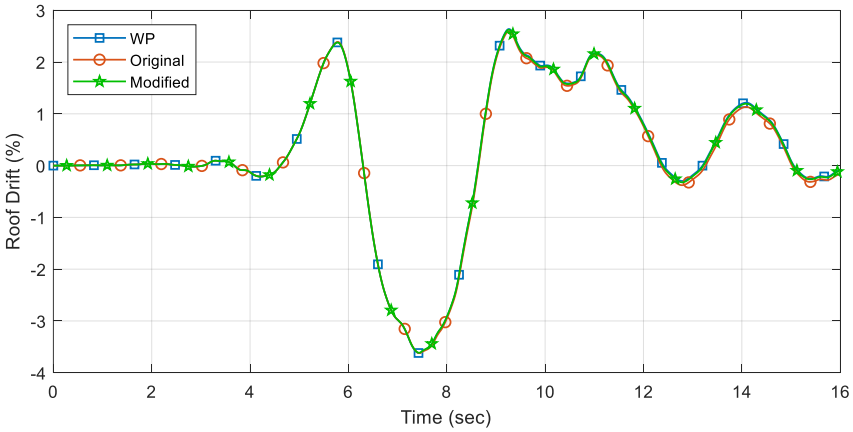

Fig. 8 – Roof displacement time histories.

The differences in the results using the different damping models become noticeable when local responses are examined. Fig.9 shows the maximum inter-storey shear normalized to floor weight.

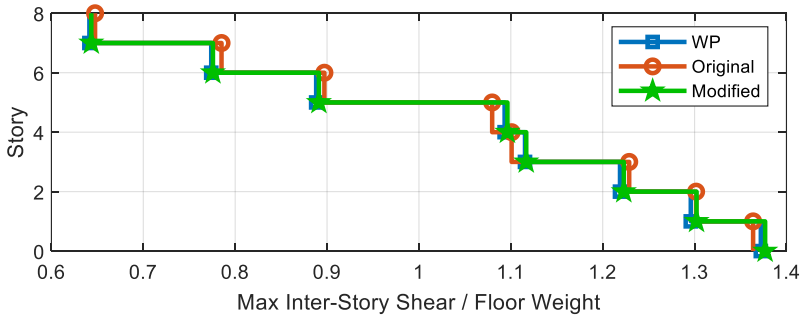

Fig. 9 – Maximum inter-storey shear.

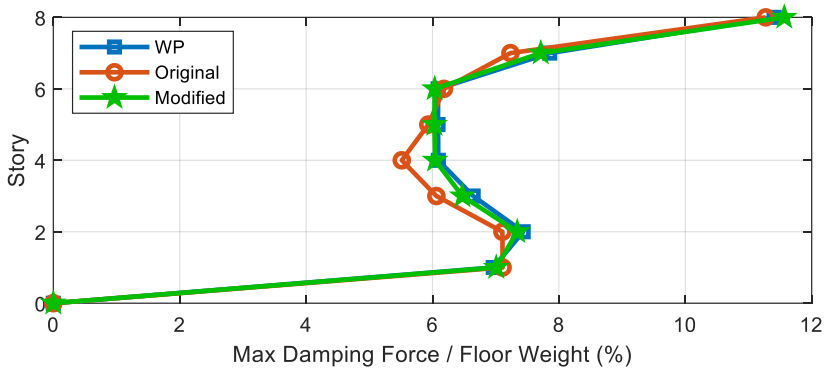

Fig. 10 – Maximum damping force.

Fig.10 shows the maximum storey damping forces normalized to floor weight. These local responses are clearly affected by the second mode with significant contributions and, therefore, show noticeable differences when the damping ratio at the second mode is not consistently matched. The original model with a lower damping ratio for the second mode gives the maximum inter-storey shear and damping forces different from using the Wilson-Penzien model. With the success in generating a steep transition and a correct damping ratio for the second mode, the modified model shows a result consistent with using the Wilson-Penzien model.

The above discussions show that, it is important for a damping model to be able to generate a damping ratio curve faithful to the requirement, which is a step function in this case. An incorrect representation would lead to noticeable errors in local response.

6. Conclusions

A new damping model, modified from the original damping model recently proposed by the same author, has been presented in this paper. This modified damping model allows its frequency bandwidth to be adjusted by using a parameter n_p. The bandwidth becomes smaller and smaller with a larger and larger n_p.

With this additional parameter, the modified model becomes more versatile in matching a damping ratio curve that has its value changes drastically over a short frequency interval. It could also generate a step distribution of damping ratio, which is sometimes considered to allow for having a lower damping for lower modes, while keeping a higher damping for higher modes.

Examples have been given to demonstrate the accuracy of the modified model in comparison against the original model and the Wilson-Penzien model. The comparison shows that the modified model, with the ability to represent the step distribution with a steeper slope at the transition, gives a result consistent to the Wilson-Penzien model for both global and local responses. On the contrary, the original model, with a gentler slope at the transition that compromises the damping ratio of the second mode, results in errors for local response.

7. References

[1] PEER/ATC (2010): *Modeling and acceptance criteria for seismic design and analysis of tall buildings*, Peer/ATC 72-1.

[2] Chopra AK (2012): *Dynamics of structures: theory and applications to earthquake engineering*. Prentice Hall, Upper Saddle River, N.J, 4th edition.

[3] Rayleigh JWSB (1896): *The theory of sound*. Macmillan, Volume 2.

[4] Caughey T (1960): Classical normal modes in damped linear dynamic systems. *Journal of Applied Mechanics*, **27**, 269–271.

[5] Wilson E, PenzienJ (1972): Evaluation of orthogonal damping matrices. *International Journal for Numerical Methods in Engineering*, **4**, 5–10.

[6] Luco JE (2008): A note on classical damping matrices. *Earthquake Engineering & Structural Dynamics*, **37**, 615–626.

[7] Chopra AK, McKenna F (2016): Modeling viscous damping in nonlinear response history analysis of buildings for earthquake excitation. Earthquake Engineering & Structural Dynamics, **45**, 193–211.

[8] Lee C-L (2019): A novel damping model for earthquake induced structural response simulation. *Proceedings of the 2019 Pacific Conference on Earthquake Engineering and Annual NZSEE Conference*, Auckland, New Zealand, 4-6 April 2019, 4C.07.

[9] Lee C-L (2019): Efficient proportional damping model for simulating seismic response of large-scale structures. *7th International Conference on Computational Methods in Structural Dynamics and Earthquake Engineering*, Crete, Greece, 24-26 June.

[10] Lee C-L (2020): Proportional Viscous Damping Model for Matching Damping Ratios. *Engineering Structures*, in press.

[11] Clough R, Penzien J (2003): *Dynamics of structures*, Computers and Structures, Inc, Berkeley, California, 3rd edition.

[12] Gibbs JW (1898): Fourier's Series. *Nature*, 59 (1522), 200.

[13] Gibbs JW (1899): Fourier's Series. *Nature*, 59 (1539), 606.

[14] Giberson MF (1967): The response of nonlinear multi-story structures subjected to earthquake excitation. *Ph.D. thesis*, Engineering and Applied Science, California Institute of technology.

[15] Filippou FC, Constantinides M (2004): FEDEASLab Getting Started Guide and Simulation Examples. *Technical report NEESgrid-2004-22*, Civil and Environmental Eng. Dept. University of California at Berkeley.

